

Evaluation of Human Health Risks Associated with Selected Heavy Metal Exposure from Fumarolic Condensates in Mt. Suswa, Kenya

Gideon Yator*, Jackson John Kitetu, Caroline Chepkirui

Department of Physical and Biological Sciences, Kabarak University, P.O. Private Bag 20157, Nakuru - Kenya.

* Corresponding author

DOI: <https://dx.doi.org/10.51244/IJRSI.2025.1210000078>

Received: 02 October 2025; Accepted: 08 October 2025; Published: 04 November 2025

ABSTRACT

Fumarolic condensates in volcanic terrains often serve as critical water sources for nearby communities but may contain toxic heavy metals mobilized through magmatic degassing and hydrothermal leaching. This study evaluated the potential human health risks associated with exposure to selected heavy metals (arsenic (As), cadmium (Cd), lead (Pb), and mercury (Hg)) in fumarolic condensates from Mt. Suswa, Kenya. Condensate samples were collected from ten modified fumarolic vents actively used by local residents and analyzed using an Agilent 5110 ICP-OES for trace-metal quantification. The mean concentrations of As (3.86 ppb), Pb (1.43 ppb), and Cd (0.85 ppb) were all below World Health Organization (2022) and NEMA (2024) limits, while Hg remained undetected in all samples. The Heavy Metal Pollution Index (HPI) and Heavy Metal Evaluation Index (HEI) indicated moderate contamination (mean HPI = 20.46 ± 12.75 ; HEI = 0.70 ± 0.28), with higher enrichment observed in inner-caldera fumaroles, reflecting stronger magmatic influence. Health-risk assessment following USEPA (2011) methodology showed that non-carcinogenic hazard quotients (HQ) for As and Cd were below unity for both adults and children, though relatively higher in children, indicating greater susceptibility to chronic exposure. The carcinogenic risk (CR) for As ranged from 9.98×10^{-5} (F2) to 1.00×10^{-4} (F4) for adults and 9.78×10^{-5} (F10) to 1.92×10^{-5} (F6) for children, with the former slightly exceeding the upper USEPA threshold (10^{-6} – 10^{-4}), suggesting a low but notable lifetime cancer probability from prolonged exposure. Although overall contamination levels were low, localized enrichment and cumulative exposure may pose health risks to vulnerable populations. These findings underscore the importance of continuous monitoring, community education, and sustainable mitigation strategies such as alternative safe-water supplies and affordable point-of-use treatment technologies in geothermal-affected regions.

Keywords: Mt. Suswa, fumarolic condensates, heavy metals, human health risk

INTRODUCTION

Geothermal and volcanic regions are characterized by extensive hydrothermal activity that releases gases and condensates enriched with various trace elements and heavy metals. These condensates often provide vital freshwater sources for surrounding communities, especially in arid or semi-arid volcanic terrains where alternative supplies are limited. However, geothermal fluids commonly carry toxic metals such as arsenic (As), cadmium (Cd), lead (Pb), and mercury (Hg), which originate from magmatic degassing, mineral dissolution, and rock–water interactions (Ayari et al., 2023; Yao et al., 2024). When these metals enter fumarolic waters, they can accumulate in biota or drinking-water systems, posing long-term health threats even at trace concentrations (Durowoju et al., 2020; Sunguti et al., 2024)

Globally, geothermal fields such as Rotorua (New Zealand), Aluto–Langano (Ethiopia), and Larderello (Italy) have been shown to contain elevated levels of As, Cd, and Pb in geothermal discharges that exceed international drinking-water limits (Morales-deAvila et al., 2023; Sanjuan, 2024). Chronic ingestion or inhalation of these metals has been linked to systemic and carcinogenic health effects, including skin lesions and keratosis, renal tubular dysfunction, neurological impairment, and various cancers (Charkiewicz et al., 2023; kaur et al., 2024).

The World Health Organization (WHO, 2022) and USEPA, (2011) have established permissible guideline values and risk-assessment frameworks to quantify both non-carcinogenic (hazard quotient, HQ) and carcinogenic (cancer risk, CR) indices for metals of public-health concern.

Within Africa, the East African Rift System (EARS) holds vast geothermal potential, with Kenya, Ethiopia, and Tanzania at the forefront of its development (Elbarbary et al., 2022). However, comprehensive research on heavy metal contamination and its health risks from these geothermal sources are limited, leaving a significant knowledge gap in understanding the environmental impacts of geothermal activities in the region. In Kenya, fumarolic and hydrothermal features occur widely along the Central Kenya Rift, including Olkaria, Eburru, Longonot, Menengai, and Mt. Suswa (Mangi, 2016).

Mt. Suswa, located in the southern segment of the Kenya Rift Valley approximately 120 km northwest of Nairobi, is characterized by a unique double-caldera structure with active fumaroles and extensive geothermal manifestations. Communities residing around Mt. Suswa depend heavily on condensed geothermal steam from fumarolic vents for domestic water needs (Mohamud, 2013). Beyond its geothermal potential, the study area supports Maasai pastoralist livelihoods and possesses high ecological and cultural significance, making the balance between geothermal development, environmental protection, and community health critically important. Local residents use fumarolic condensates for drinking, bathing, cooking, and watering livestock, thereby increasing potential exposure to heavy-metal contaminants (Masikonte, 2020). Yet, systematic evaluations of heavy-metal contamination and associated health impacts in the Mt. Suswa area remain limited or nonexistent. Consequently, baseline data to support environmental monitoring, community health protection, and sustainable geothermal resource management are lacking.

This study therefore aimed to evaluate the potential human health risks associated with exposure to selected heavy metals (As, Cd, Pb, and Hg) in fumarolic condensates from Mt. Suswa, Kenya. By linking geochemical data with quantitative health-risk metrics, the study provides essential baseline information for the Mt. Suswa geothermal prospect and enhances understanding of heavy-metal exposure pathways within the broader East African Rift System.

METHODOLOGY

Study Area and Geology

Mt. Suswa, the southernmost Quaternary volcano along the axis of the Central Kenya Rift, is bounded by latitudes 1.00°S–1.18°S and longitudes 36.13°E–36.33°E. It lies approximately 120 km northwest of Nairobi and represents one of Kenya's most distinctive volcanic structures (Fig. 1). The mountain is a Quaternary trachytic shield volcano characterized by a unique double-caldera system consisting of an inner caldera, about 4 km in diameter, enclosed within an outer caldera measuring roughly 12 × 8 km, with the rim reaching an elevation of 1,890 m above sea level. The volcano rises nearly 800 m above the Rift Valley floor, attaining a maximum elevation of 2,356 m, and covers an estimated area of over 700 km² (Nyairo et al., 2014).

Geologically, Mt. Suswa is composed predominantly of trachytic, and basaltic lavas, interbedded with tuffs, pyroclastic deposits, and volcanic breccias. These lithologies form the structural and hydrological framework that hosts a vapor-dominated geothermal system. Fumarolic activity is concentrated along ring faults and fracture zones associated with caldera collapse and resurgence (Mohamud, 2013).

The broader Mt. Suswa prospect exhibits active fumarolic emissions and the surrounding terrain is semi-arid and inhabited primarily by Maasai pastoralist communities, who rely heavily on condensed fumarolic steam for domestic water use due to limited access to conventional freshwater sources.

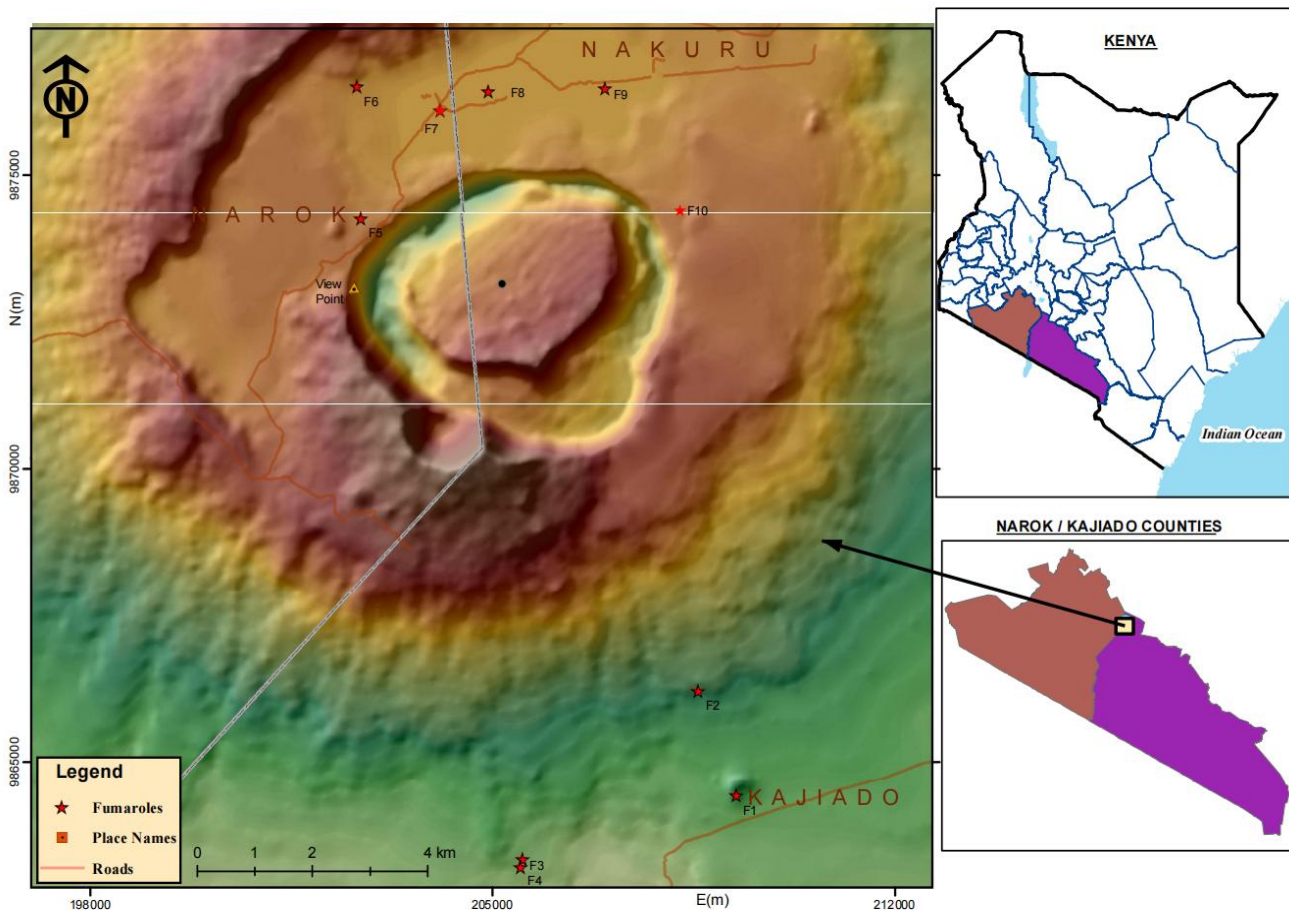


Fig 1: Location and sampling sites of fumarolic vents in the Mt. Suswa area

Sample Collection and Preparation

Condensate samples were obtained from ten (10) modified fumarolic vents actively used by the local community within the Mt. Suswa geothermal area. Sampling was conducted during the early morning hours to minimize evaporation losses and airborne contamination. At each site, condensates were collected directly from condensation pipes into pre-acid-washed 500 mL high-density polyethylene (HDPE) bottles.

To ensure analytical reliability, duplicate samples were collected from each fumarole during every sampling event. One bottle was immediately acidified in the field with 1 mL of concentrated nitric acid (HNO_3) to lower the pH to < 2 , preventing metal adsorption onto container walls and preserving dissolved elements for trace-metal analysis. The second bottle was used for in situ measurement of physico-chemical parameters, including temperature ($^{\circ}\text{C}$), pH, electrical conductivity (EC, $\mu\text{S}/\text{cm}$), and total dissolved solids (TDS, mg/L).

Temperature measurements were performed using a Hanna HI-935002 thermocouple thermometer (Woonsocket, USA), while pH and EC were determined using a Jenway 430 pH/Conductivity meter (London, UK). All samples were carefully sealed, labeled, and stored at 4°C in insulated coolers to preserve their integrity prior to laboratory analysis.

Sample Analysis

Water Quality Assessment

Basic physico-chemical parameters (pH, EC, TDS) were analyzed following the American Public Health Association (APHA, 2022) standard methods. Results were compared against World Health Organization (WHO, 2022) and Kenya's National Environment Management Authority (NEMA, 2024) drinking-water guideline values to assess compliance and suitability for domestic use.

Heavy-Metal Analysis and Quality Control

Concentrations of arsenic (As), lead (Pb), cadmium (Cd), and mercury (Hg) were quantified using an Agilent 5110 Inductively Coupled Plasma–Optical Emission Spectrometer (ICP-OES) at the Kenya Bureau of Standards (KEBS) Laboratory. Calibration standards (0, 5, 10, 25, 50 ppb) were prepared from certified 1000 mg/L stock solutions. Instrument calibration curves exhibited correlation coefficients (R^2) ≥ 0.999 . Analytical precision and accuracy were verified through reagent blanks, matrix spikes, and triplicate determinations. Method detection limits (MDLs) were 0.01 $\mu\text{g/L}$ for As, 0.02 $\mu\text{g/L}$ for Pb, 0.01 $\mu\text{g/L}$ for Cd, and 0.05 $\mu\text{g/L}$ for Hg. Recovery rates ranged from 98% to 103%, ensuring analytical reliability.

Compositional Indices

Heavy Metal Pollution Index (HPI)

The Heavy Metal Pollution Index (HPI) was used to assess the overall quality of the fumarolic condensates based on the combined effect of multiple heavy metals. The HPI provides a composite measure that indicates the degree of heavy-metal contamination relative to standard permissible limits. The HPI was computed using the weighted arithmetic mean model as described by Eldaw et al., (2020) ;

$$HPI = \frac{\sum(W_i Q_i)}{\sum W_i} \dots\dots\dots (1)$$

where:

$$Q_i = \frac{(M_i - I_i)}{(S_i - I_i)} \times 100 \dots\dots\dots (2)$$

and

M_i = Measured concentration of the i^{th} metal ($\mu\text{g/L}$),

I_i = Ideal value (zero for all metals),

S_i = Standard permissible value (WHO, 2022),

W_i = Unit weight assigned to each metal, inversely proportional to S_i .

$$W_i = \frac{K}{S_i} \dots\dots\dots (3)$$

where K is a constant of proportionality ensuring normalization of the weighting factors.

Interpretation of the computed HPI values was based on established threshold ranges, where:

HPI < 50: low heavy-metal pollution (acceptable quality)

HPI = 50–100: moderate contamination

HPI > 100: high contamination or potential health concern

(Ahmed et al., 2023; Kumar & Maurya, 2025)

Heavy Metal Evaluation Index (HEI)

The Heavy Metal Evaluation Index (HEI) was also applied to assess the cumulative contamination level of the fumarolic condensates by integrating the concentrations of all analyzed metals relative to their respective permissible limits. This index provides a straightforward measure of overall heavy-metal load within a sample, reflecting both the magnitude and collective contribution of multiple contaminants. The HEI was computed following the approach of Braich & Jassal, (2021), as expressed by:

$$HEI = \sum \frac{C_i}{S_i} \dots\dots\dots (4)$$

where

C_i = Measured concentration of the i^{th} metal ($\mu\text{g/L}$),

S_i = Corresponding standard permissible concentration(WHO, 2022).

Interpretation of HEI values was based on the following classification criteria:

HEI < 1: low contamination (negligible impact)

HEI = 1–10: moderate contamination

HEI > 10: high contamination (significant pollution potential)

These indices were applied to determine the overall extent of metal enrichment and to identify spatial variations in contamination intensity, aligning with recent studies that have employed HPI and HEI to evaluate multi-metal pollution patterns and cumulative water quality degradation in aquatic environments (Tokatli, 2024; Wu et al., 2024)

Human Health Risk Assessment

The health risk assessment was conducted using the United States Environmental Protection Agency (USEPA, 2011) risk assessment framework. Non-carcinogenic risks were evaluated using the Hazard Quotient (HQ) for individual metals and the Hazard Index (HI) for cumulative effects, while carcinogenic risks were quantified using the Lifetime Cancer Risk (LCR) model. The exposure pathways considered in this analysis included both ingestion and dermal absorption, as these represent the primary routes of human exposure to fumarolic condensates in the Suswa community. All the parameters for calculations are summarized in Table 1 below;

(i) Ingestion Pathway

The Lifetime Cancer Risk via ingestion was estimated using Equation 8:

$$LCR_{\text{ingestion}} = EDI_{\text{ingestion}} + SF \dots\dots\dots (5)$$

Where:

$LCR_{\text{ingestion}}$ = Lifetime Cancer Risk from ingestion exposure.

$EDI_{\text{ingestion}}$ = Estimated Daily Intake via ingestion (mg/kg/day), calculated using Equation 6

$$EDI_{\text{ingestion}} = \frac{C_W \times IR \times EF \times ED}{BW \times AT} \dots\dots\dots (6)$$

(ii) Dermal Pathway

The Lifetime Cancer Risk via dermal absorption was calculated using Equation 7 and 8:

$$LCR_{\text{dermal}} = EDI_{\text{dermal}} + SF \dots\dots\dots (7)$$

- LCR_{dermal} = Lifetime Cancer Risk from dermal exposure.

- EDI_{dermal} = Estimated Daily Intake via dermal absorption (mg/kg/day), calculated using:

$$EDI_{\text{dermal}} = \frac{C_W \times SA \times KP \times ET \times EF \times ED \times CF}{BW \times AT} \dots\dots\dots (8)$$

Table 1: Parameters and Their Sources for HPI, HEI, HQ, HI, and CR Calculations

Parameter	Symbol	Unit	Description	Source
Metal concentration	(C_i) or (M_i)	$\mu\text{g/L}$ (ppb)	Measured concentration of metal (As, Cd, Pb, Hg) in fumarolic condensates	This study (Agilent 5110 ICP-OES results)
Standard permissible limit	(S_i)	$\mu\text{g/L}$	WHO and NEMA guideline values for safe drinking water	WHO (2022); NEMA (2019)
Ideal value	(I_i)	$\mu\text{g/L}$	Ideal (zero) concentration for metals in pure water	(Kowalska et al., 2018); USEPA (2011)
Unit weight	(W_i)	—	Weight assigned inversely proportional to permissible limit $((W_i = 1/ S_i))$	(Kowalska et al., 2018)
Sub-index for HPI	(Q_i)	—	Metal quality rating; $(Q_i = ((M_i - I_i)/(S_i - I_i)) \times 100)$	(Kowalska et al., 2018)
Heavy Metal Pollution Index	HPI	—	Overall degree of heavy metal contamination	(Anitha et al., 2021)
Heavy Metal Evaluation Index	HEI	—	Summation of ratios of concentration to standard limits; $(HEI = \sum (C_i/S_i))$	(Prasad & Bose, 2001)
Estimated Daily Intake	EDI	mg/kg/day	Intake of metal through ingestion pathway; $(EDI = (C_w \times IR \times EF \times ED)/(BW \times AT))$	USEPA (2011)
Ingestion rate	IR	L/day	Volume of condensate consumed per day (2 for adults; 1 for children)	USEPA (2011)
Exposure frequency	EF	days/year	Days per year of exposure (365)	USEPA (2011)
Exposure duration	ED	years	Period of exposure (30 for adults; 6 for children)	USEPA (2011)
Body weight	BW	kg	Average human body mass (70 for adults; 15 for children)	USEPA (2011)
Averaging time (non-carcinogenic)	AT_n	days	$ED \times 365$	USEPA (2011)
Averaging time (carcinogenic)	AT_c	days	70×365 (lifetime exposure)	USEPA (2011)
Oral reference dose	RfD	mg/kg/day	Acceptable daily intake for As = 3×10^{-4} , Cd = 1×10^{-3}	USEPA (2011)

Cancer slope factor	CSF	(mg/kg/day) ⁻¹	Factor for carcinogenic potential; As = 1.5; Cd = 6.3	USEPA (2011)
Hazard Quotient	HQ	—	Ratio of EDI to RfD; (HQ = EDI / RfD)	USEPA (2011)
Hazard Index	HI	—	Sum of HQs for multiple metals; (HI = \sum HQ _i)	USEPA (2011)
Carcinogenic Risk	CR	—	Lifetime probability of cancer; (CR = EDI × CSF)	USEPA (2011); Rahman et al. (2019)

Total Cancer Risk and Interpretation

The overall cumulative cancer risk from exposure to carcinogenic heavy metals in fumarolic condensates was estimated by summing the Lifetime Cancer Risks (LCR) from all relevant pathways, namely ingestion and dermal absorption. This total risk provided a comprehensive estimate of the lifetime probability of developing cancer as a result of chronic exposure to contaminants in the fumarolic condensates. The calculation was performed using Equation 9:

$$LCR_{Total} = LCR_{ingestion} + LCR_{dermal} \dots \dots \dots (9)$$

Where:

- LCR_{Total} : Total Lifetime Cancer Risk (unitless probability).
- $LCR_{ingestion}$: Lifetime Cancer Risk from ingestion exposure.
- LCR_{dermal} : Lifetime Cancer Risk from dermal exposure.

The total cancer risk therefore represented the cumulative probability of an individual developing cancer over a lifetime due to simultaneous exposure to heavy metals through both ingestion and dermal pathways (Raad et al., 2021;USEPA, 2011)

Non-carcinogenic risks were assessed using the Hazard Quotient (HQ) and Hazard Index (HI). An HQ or HI value greater than one (>1) indicated potential health concerns associated with exposure to a given contaminant or combined contaminants. Carcinogenic risks, expressed as LCR values, were interpreted against the thresholds recommended by USEPA, (2011). Risks below $LCR < 1 \times 10^{-6}$ were considered negligible, while risks $LCR \geq 1 \times 10^{-4}$ were considered unacceptable. Risks falling within the range of $10^{-6} \leq LCR < 10^{-4}$ were regarded as tolerable but requiring careful monitoring and, where possible, mitigation measures (Demissie et al., 2024; USEPA, 2011).

Non-carcinogenic risk

$$HQ_i = \frac{EDI_i}{RfD_i} \dots \dots \dots (10)$$

$$LCR_{Total} = \sum HQ_i \dots \dots \dots (11)$$

Where RfD_i is the reference dose for metal *i*. HQ or HI > 1 indicates potential concern.

Statistical Analysis

All analyses were conducted in triplicate, and results were expressed as mean ± standard deviation (SD). Quantitative data obtained from laboratory and field analyses were subjected to descriptive statistics (mean,

range, and standard deviation) to summarize the contamination levels and physico-chemical characteristics of fumarolic condensates across different vents within the study area.

To evaluate variations in contaminant concentrations among fumarolic vents, inferential statistical tests, including a one-way analysis of variance (ANOVA), were applied where assumptions of normality and homogeneity of variance were satisfied (Mukwevho et al., 2025). Statistical analyses were performed using SPSS version 26.0 and significance was determined at $p < 0.05$.

RESULTS AND INTERPRETATION

Heavy Metal Concentration in Fumarolic Condensates

The physico-chemical parameters and heavy-metal concentrations of fumarolic condensates from the Mt. Suswa geothermal area are summarized in Table 2 below. The condensates exhibited near-neutral to slightly acidic pH values (5.52–7.26; mean = 6.50 ± 0.42), consistent with weakly acidic conditions resulting from the dissolution of magmatic gases such as CO_2 and SO_2 in condensate water. Temperatures ranged from 51.4 °C to 74.3 °C (mean = 63.2 ± 7.2 °C), with higher temperatures observed in vents located within the inner caldera. Electrical conductivity (EC) and total dissolved solids (TDS) varied between 5.16–51.22 $\mu\text{S}/\text{cm}$ and 2.58–25.6 ppm, respectively, indicating low mineralization typical of dilute hydrothermal condensates formed by steam condensation of meteoric water.

The selected heavy-metal concentrations showed noticeable spatial variability (Table 2). Arsenic (As) ranged from 2.24 to 5.49 ppb (mean = 3.86 ± 1.05 ppb), while lead (Pb) ranged between 0.95 and 1.98 ppb (mean = 1.43 ± 0.31 ppb). Cadmium (Cd) concentrations were generally low, detected only in six fumaroles (0.39–1.41 ppb; mean = 0.84 ± 0.34 ppb), whereas mercury (Hg) was below detection limits in all samples. All mean concentrations were below the WHO (2022) and NEMA (2024) permissible limits for drinking water, implying that fumarolic condensates were of acceptable chemical quality despite minor geogenic enrichment.

Spatially, fumaroles F9 and F10 exhibited the highest concentrations of As and Cd, corresponding to sites of elevated temperature and vapor discharge near the inner-caldera vent system. This spatial pattern suggests that elevated temperature enhances rock-steam interaction and leaching of volatile trace elements from hydrothermally altered minerals.

Table 2: Physico-chemical parameters and heavy-metal concentrations (mean \pm RSD %) in fumarolic condensates from the Mt. Suswa geothermal area.

S. No	Sample Map	Latitude	Longitude	pH/T°C	EC	TDS	As	Pb	Cd	Hg
					μS	(ppm \pm %)	Mean \pm SD (ppb \pm %)			
F1	F1	-1.227821	36.388119	7.19/51.4	14.72	7.36	4.86 ± 0.20	1.42 ± 0.09	ND	ND
F2	F2	-1.211764	36.382253	7.26/58.2	5.16	2.58	3.21 ± 0.23	1.30 ± 0.07	0.53 ± 0.06	ND
F3	F3	-1.237729	36.354751	6.68/53.1	13.07	6.58	4.94 ± 0.10	1.53 ± 0.17	0.82 ± 0.09	ND
F4	F4	-1.238985	36.354498	6.94/64.6	17.01	8.52	3.82 ± 0.34	1.38 ± 0.11	0.39 ± 0.02	ND
F5	F6	-1.185491	36.32553	6.36/64.1	18.73	9.37	2.55 ± 0.28	1.35 ± 0.05	ND	ND
F6	F7	-1.138952	36.329659	7.12/63.2	17.33	8.67	2.24 ± 0.16	0.95 ± 0.13	ND	ND

F7	F10	-1.118744	36.328995	6.44/54.4	11.92	5.96	3.13 ± 0.06	1.62 ± 0.05	ND	ND
F8	F14	-1.12676	36.338155	6.19/71.2	22.41	11.2	3.32 ± 0.10	1.98 ± 0.08	0.68 ± 0.02	ND
F9	F18	-1.124473	36.338121	6.43/73.5	51.22	25.6	5.07 ± 0.46	1.27 ± 0.08	1.22 ± 0.05	ND
F10	F20	-1.12238	36.34202	5.52/74.3	21.15	10.54	5.49 ± 0.22	1.52 ± 0.05	1.41 ± 0.11	ND
NEMA Limit				6.5–8.5	NS	1200	10	50	10	1
WHO Limit				6.5–8.0	NS	1000	10	10	3	5

Note: Values are represented as Mean ±SD from triplicate analyses; ND = Not Detected; NS = Not Specified. Hg was below the detection limit of 0.01 ppb in all samples.

The variability in trace-metal concentrations across fumaroles indicates the influence of localized geothermal intensity and fluid-rock interactions, warranting evaluation of potential health implications through exposure and risk indices.

Estimated Daily Intake (EDI)

The estimated daily intake (EDI) quantifies the potential exposure of individuals consuming fumarolic condensates. Using USEPA (2011) exposure parameters, the EDI for adults ranged from 1.0×10^{-5} to 1.2×10^{-4} mg/kg/day for As and 0.5×10^{-5} to 4.3×10^{-5} mg/kg/day for Pb as shown in Table 3 below. Children had proportionally higher EDI values, approximately 2.5–3 times those of adults due to lower body mass and higher intake rates per kilogram body weight.

All EDI values were below their corresponding reference doses (RfD), implying minimal immediate toxicological risk, although As exposure in children approached the RfD threshold.

Table 3: Estimated Daily Intake (EDI; mg/kg/day) of heavy metals in fumarolic condensates.

Metal	Adults	Children	RfD (mg/kg/day)	Interpretation
As	1.2×10^{-4}	3.0×10^{-4}	3.0×10^{-4}	Marginal for children
Pb	4.3×10^{-5}	1.1×10^{-4}	3.5×10^{-3}	Safe
Cd	1.6×10^{-5}	4.0×10^{-5}	1.0×10^{-3}	Safe
Hg	ND	ND	3.0×10^{-4}	Not detected

Human Health Risk Assessment

Non-Carcinogenic Risk (HQ and HI)

The Hazard Quotient (HQ) and cumulative Hazard Index (HI) were computed to assess non-carcinogenic risks associated with ingestion of fumarolic condensates. All HQ values for adults were below unity, indicating no significant health effects from individual metals. In children, HQ values for arsenic ranged from 0.45 to 0.98 in high-temperature fumaroles (F9 and F10), suggesting marginal concern. The mean HI values of 0.36 for adults and 0.80 for children were both below the critical threshold of 1, denoting negligible to low health risk. However, the higher HQ values in children reflect their greater vulnerability due to lower body mass and higher water intake per kilogram of body weight.

These findings are summarized in Table 4, which presents the range and mean HQ values for each metal and the cumulative HI for both adults and children. The results confirm that exposure to arsenic poses the greatest relative contribution to non-carcinogenic risk, particularly among children living near high-temperature fumaroles.

Table 4: Hazard Quotient (HQ) and Cumulative Hazard Quotient (CHQ) for adults and children in fumarolic condensates from Mt. Suswa.

Metal	Min HQ (Adults)	Max HQ (Adults)	Mean HQ (Adults)	Min HQ (Child)	Max HQ (Child)	Mean HQ (Child)	Interpretation
As	0.21	0.45	0.32	0.45	0.98	0.68	Marginal risk in hot vents for children; safe for adults
Pb	0.01	0.02	0.02	0.05	0.12	0.08	Safe for both groups
Cd	0.01	0.03	0.02	0.02	0.05	0.04	Safe for both groups
HI (Σ HQ)	—	—	0.36	—	—	0.8	Within acceptable limit for adults; near threshold for children

Carcinogenic Risk (CR)

Carcinogenic risk, expressed as the Lifetime Cancer Risk (LCR), was assessed for arsenic (As) and cadmium (Cd) using their respective cancer slope factors of 1.5 and 6.3 ($\text{mg kg}^{-1} \text{ day}^{-1}$)⁻¹ as prescribed by the United States Environmental Protection Agency (USEPA, 2011). The computed LCR values for adults ranged from 4.1×10^{-5} to 2.1×10^{-4} , whereas those for children varied between 1.9×10^{-5} and 9.8×10^{-5} . Most of these values fall within the USEPA's acceptable carcinogenic risk range (10^{-6} – 10^{-4}), indicating generally low health risks associated with long-term exposure to the fumarolic condensates.

As summarized in Table 5, arsenic contributed the highest proportion of the total cancer risk across all fumaroles, reflecting its elevated geochemical mobility and strong affinity for geothermal vapor transport. Cadmium played a lesser but noticeable role in enhancing total risk where it was detectable (notably at F3, F8–F10). The mean total LCR for adults (7.6×10^{-5}) and for children (1.8×10^{-4}) remained within or marginally above the acceptable threshold, with the highest values recorded at fumaroles F9 and F10, both located in the inner caldera where elevated temperature and gas flux intensify trace-metal mobilization.

The findings suggest that the carcinogenic risk from fumarolic condensates in Mt. Suswa is generally acceptable, though localized elevated LCRs at hot vents highlight the need for continued monitoring and community-level mitigation such as point-of-use treatment, controlled exposure, and public awareness programs.

Table 5: Lifetime Cancer Risk (LCR) of heavy metals in fumarolic condensates for adults and children by sampling site.

Fumarole	As (Adults)	Cd (Adults)	LCR _{Total} (Adults)	As (Child)	Cd (Child)	LCR _{Total} (Child)	Interpretation
F1	8.93×10^{-5}	0	8.93×10^{-5}	4.17×10^{-5}	0	4.17×10^{-5}	Acceptable

F2	5.90×10^{-5}	4.09×10^{-5}	9.98×10^{-5}	2.75×10^{-5}	1.91×10^{-5}	4.66×10^{-5}	Acceptable
F3	9.07×10^{-5}	6.33×10^{-5}	1.54×10^{-4}	4.23×10^{-5}	2.95×10^{-5}	7.19×10^{-5}	Elevated concern
F4	7.02×10^{-5}	3.01×10^{-5}	1.00×10^{-4}	3.27×10^{-5}	1.40×10^{-5}	4.68×10^{-5}	Marginal concern
F5	4.68×10^{-5}	0	4.68×10^{-5}	2.19×10^{-5}	0	2.19×10^{-5}	Acceptable
F6	4.11×10^{-5}	0	4.11×10^{-5}	1.92×10^{-5}	0	1.92×10^{-5}	Acceptable
F7	5.75×10^{-5}	0	5.75×10^{-5}	2.68×10^{-5}	0	2.68×10^{-5}	Acceptable
F8	6.10×10^{-5}	5.25×10^{-5}	1.13×10^{-4}	2.85×10^{-5}	2.45×10^{-5}	5.29×10^{-5}	Elevated concern
F9	9.31×10^{-5}	9.41×10^{-5}	1.87×10^{-4}	4.35×10^{-5}	4.39×10^{-5}	8.74×10^{-5}	Elevated concern
F10	1.01×10^{-4}	1.09×10^{-4}	2.10×10^{-4}	4.71×10^{-5}	5.08×10^{-5}	9.78×10^{-5}	Elevated concern
Mean	6.90×10^{-5}	7.70×10^{-6}	7.60×10^{-5}	1.60×10^{-4}	2.10×10^{-5}	1.80×10^{-4}	Generally acceptable; marginal at hot vents

Compositional Indices (HPI and HEI)

The Heavy-Metal Pollution Index (HPI) and Heavy-Metal Evaluation Index (HEI) were computed using the WHO (2022) permissible limits for arsenic (10 µg/L), lead (10 µg/L), and cadmium (3 µg/L) to evaluate the cumulative metal burden in fumarolic condensates. The HPI values ranged from 5.98 to 42.57, all below the critical threshold of 50, indicating low overall contamination. Correspondingly, HEI values varied between 0.32 and 1.17, suggesting low to moderate heavy-metal load across the fumarolic field.

As summarized in Table 6, fumaroles F9 and F10 exhibited the highest HPI and HEI values, corresponding to localized enrichment of arsenic and cadmium in high-temperature vents. These sites are situated near the inner caldera, where intense geothermal activity enhances rock–steam interactions and metal volatilization. The mean HPI (20.76) and mean HEI (0.74) classify the fumarolic condensates as acceptable in quality, though with minor geogenic enrichment indicative of hydrothermal contribution. The overall results demonstrate spatial variability consistent with temperature gradients and vapor flux intensity within the Suswa geothermal system.

Table 6: Heavy-Metal Pollution Index (HPI) and Heavy-Metal Evaluation Index (HEI) for fumarolic condensates (Mt. Suswa).

Fumarole	HPI	HEI	Interpretation
F1	11.78	0.63	Low pollution
F2	19.53	0.63	Low pollution
F3	29.20	0.92	Low–moderate
F4	17.88	0.65	Low pollution

F5	7.31	0.39	Very low
F6	5.98	0.32	Very low
F7	8.91	0.48	Low
F8	24.12	0.76	Low–moderate
F9	37.33	1.04	Moderate
F10	42.57	1.17	Moderate
Mean	20.46± 12.75	0.70± 0.28	Low–moderate overall

The fumarolic condensates from Mt. Suswa exhibit low to moderate heavy-metal contamination, with As and Pb being the dominant elements of concern. The observed metal levels are below WHO and NEMA thresholds, confirming that the condensates are chemically suitable for domestic use after minor treatment.

However, spatially elevated HPI and HEI values in the inner-caldera fumaroles (F9 and F10) indicate localized enrichment influenced by higher temperature and prolonged water-rock interaction. Health-risk assessment revealed that non-carcinogenic risks are minimal ($HQ < 1$) but potential carcinogenic risks from As in children ($LCR \approx 1 \times 10^{-4}$) merit attention.

Overall, the integrated indices (EDI, HQ, HI, LCR, HPI, HEI) reveal that Mt. Suswa fumarolic condensates are generally of acceptable chemical quality. However, localized enrichment in As and Cd at inner-caldera vents (F9, F10) suggests elevated geothermal input, emphasizing the need for targeted monitoring and preventive exposure control.

DISCUSSION AND FINDINGS

Heavy Metal Levels in Fumaroles

The fumarolic condensates from Mt. Suswa exhibited near-neutral to slightly acidic pH values (5.52–7.26; mean = 6.50 ± 0.42), consistent with mild acidification caused by the dissolution of magmatic gases such as CO₂ and SO₂ in meteoric water. Similar processes have been documented in recent studies where fumarolic gas–water interactions generate weakly acidic condensates through magmatic gas dissolution (Obase et al., 2022; Yaguchi et al., 2025). The condensate temperatures, ranging between 51.4 °C and 74.3 °C, align with shallow steam discharge in active geothermal systems, and the particularly high temperatures in inner-caldera vents reflect intensified magmatic–hydrothermal activity (Agusto et al., 2023; Campeny et al., 2023). Electrical conductivity (EC) and total dissolved solids (TDS) varied from 5.16–51.22 µS/cm and 2.58–25.6 ppm, respectively, denoting low mineralization typical of dilute hydrothermal condensates derived from condensed steam rather than deep geothermal brines.

Concentrations of heavy metals exhibited distinct spatial variability across fumarolic vents in Mt. Suswa (Table 2). Arsenic (As) ranged between 2.24–5.49 ppb (mean = 3.86 ± 1.05 ppb), lead (Pb) varied from 0.95–1.98 ppb (mean = 1.43 ± 0.31 ppb), and cadmium (Cd) from 0.39–1.41 ppb (mean = 0.84 ± 0.34 ppb), while mercury (Hg) remained below detection limits in all samples. These trace-element concentrations are considerably lower than the WHO (2022) and NEMA (2024) permissible limits for drinking water (As = 10 µg/L, Pb = 10 µg/L, Cd = 3 µg/L), suggesting that the condensates are chemically safe despite localized enrichment within inner-caldera vents. Comparable patterns of spatial heterogeneity in fumarolic trace-metal composition have been documented in other active volcanic systems, where elevated As, Pb, and Cd near high-temperature vents are linked to vapor-phase transport and rock-steam interaction (Campeny et al., 2023; Inostroza et al., 2022; Werner et al., 2020). Such variations reflect geothermal intensity and proximity to magmatic conduits, which control the geochemical partitioning of metals within condensate fluids (Inostroza et al., 2022).

Spatially, vents F9 and F10 exhibited the highest As and Cd concentrations, co-occurring with hotter discharge zones—an association consistent with intensified rock–steam exchange and leaching of volatile trace metals from hydrothermally altered minerals under elevated thermal and vapor flux conditions (Sunguti et al., 2024). The site-specific index values at these vents (HPI = 37.33–42.57; HEI = 1.04–1.17) corroborate localized heavy-metal enrichment, whereas the overall means (HPI = 20.76; HEI = 0.74) indicate low-to-moderate pollution in line with recent applications of HPI/HEI for water-quality evaluation (Badeenezhad et al., 2023; Biedunkova & Kuznietsov, 2024). As summarized in Table 6, the fumarolic condensates at Mt. Suswa are therefore of acceptable chemical quality for potential domestic use when judged against contemporary guideline values, with only minor geogenic enrichment in inner-caldera vents; the slight acidity observed is typical of vapor-heated systems and can be mitigated by simple neutralization or blending before use (Sunguti et al., 2024; WHO, 2022).

Table 6. Comparison of Physico-Chemical Parameters with WHO and NEMA Standards

Parameter	Mean (This Study)	WHO (2022) Limit	NEMA (2024) Limit	Compliance Status
pH	5.52 – 7.26 (6.50 ± 0.42)	6.5 – 8.0	6.5 – 8.5	Acceptable (slightly acidic)
Temperature (°C)	51.4 – 74.3 (63.2 ± 7.2)	NS	NS	Typical geothermal
EC (µS/cm)	5.16 – 51.22 (19.47 ± 7.5)	1000	1200	Low mineralization
TDS (ppm)	2.58 – 25.6 (10.2 ± 3.4)	1000	1200	Excellent quality
As (ppb)	2.24 – 5.49 (3.86 ± 1.05)	10	10	Below limits
Pb (ppb)	0.95 – 1.98 (1.43 ± 0.31)	10	50	Below limits
Cd (ppb)	0.39 – 1.41 (0.84 ± 0.34)	3	10	Below limits
Hg (ppb)	ND	5	1	Not detected

Note: ND = Not Detected; NS = Not Specified.

Health Risk Assessment

Non-Carcinogenic Health Risk

Hazard Quotient (HQ) and cumulative Hazard Index (HI) values were computed for adults and children to quantify potential non-carcinogenic risks from exposure to heavy metals through ingestion of fumarolic condensates, following the U.S. Environmental Protection Agency (USEPA, 2011) guidelines. Similar approaches have recently been applied in heavy-metal risk assessments for water resources using probabilistic and deterministic exposure models (Ayaz et al., 2023; Shetty et al., 2024).

All HQ values for adults remained below unity (As = 0.32 ± 0.12 ; Pb = 0.02 ± 0.01 ; Cd = 0.02 ± 0.01), yielding a cumulative HI = 0.36. These values indicate a negligible likelihood of non-cancer health effects arising from short- or long-term exposure to the condensates. In contrast, HQ values for children were comparatively higher, particularly for arsenic (mean = 0.68 ± 0.20), producing a cumulative HI = 0.80, which approaches the critical

threshold of 1. This pattern, also reported in recent global health-risk studies (Ayaz et al., 2023; Shetty et al., 2024), reflects children’s greater vulnerability to contaminant exposure due to their higher water-intake rates and lower body weights. Elevated HQ values in the inner-caldera fumaroles (F9 and F10) imply that children living near these high-temperature vents may experience marginal but notable health risks associated with geothermal trace-metal exposure.

The heightened vulnerability of children stems from their lower body weight combined with a relatively greater ingestion rate per kilogram, leading to proportionally higher internal exposure to trace metals—this pattern has been emphasized in studies of contaminant exposure in pediatric populations (Bair, 2022; Capitão et al., 2022). Spatially, the non-carcinogenic risk indices (HQ and HI) track closely with the gradient in metal concentrations, increasing toward hotter inner-caldera vents. Although all values remain below the safety threshold, this radial trend suggests a temperature-controlled mobilization of metals and highlights zones of localized exposure risk that merit periodic surveillance (Shetty et al., 2024).

The comparative plots in Figure 2 clearly demonstrate age-related differences in susceptibility to metal exposure from fumarolic condensates. In both Hazard Quotient (HQ) and Lifetime Cancer Risk (LCR) profiles, children consistently exhibit higher values than adults, reflecting their enhanced physiological vulnerability to geogenic contaminants. This disparity arises primarily from children’s lower body weight, higher ingestion rate per unit body mass, and immature detoxification mechanisms, which collectively amplify internal doses even at comparable environmental concentrations (Jadoon et al., 2025; Okoro et al., 2025). Similar findings have been reported in recent exposure-risk studies, where non-carcinogenic and carcinogenic indices for As, Pb, and Cd were substantially higher in children than in adults consuming contaminated groundwater resources, underscoring the importance of age-specific risk evaluation and protective public health interventions (Gantayat et al., 2025).

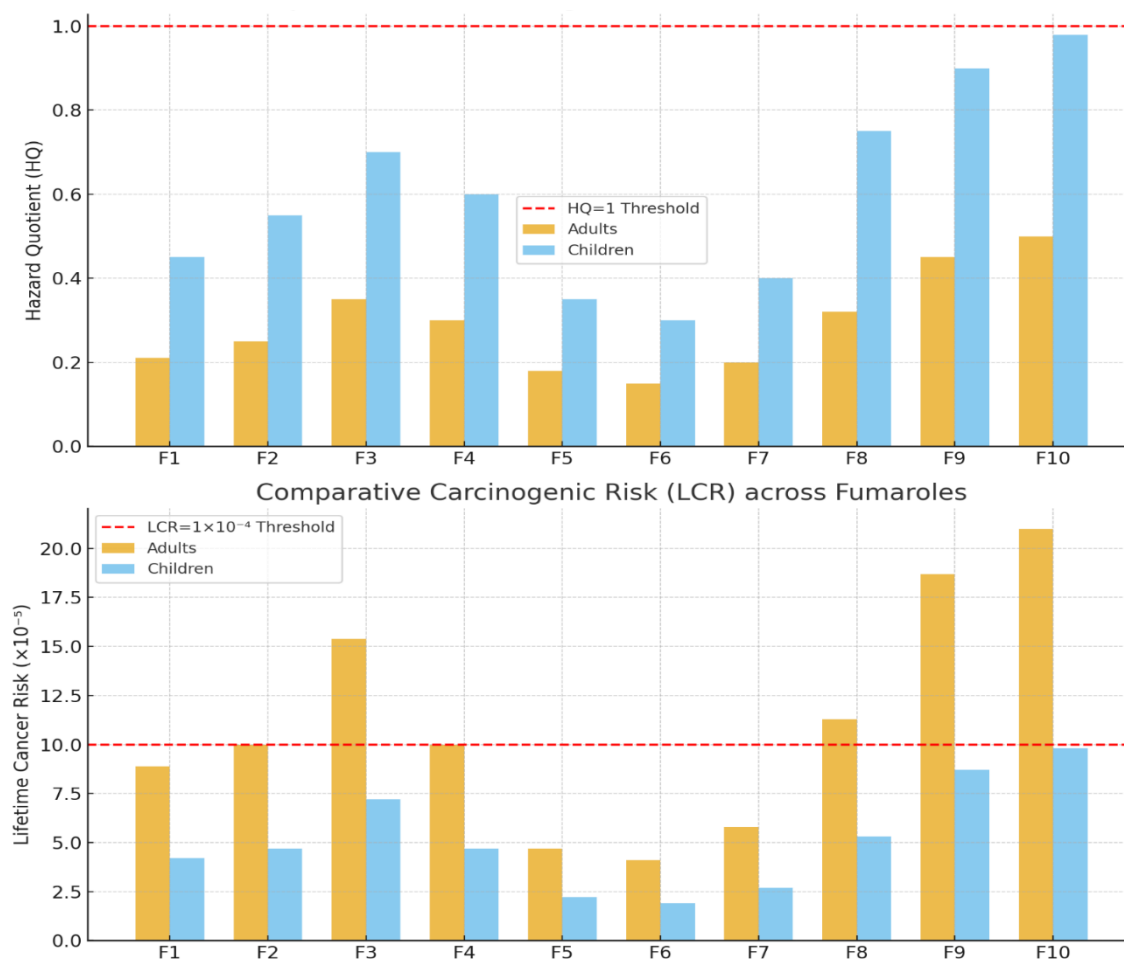


Fig 2: Comparative Non-Carcinogenic (HQ) and Carcinogenic (LCR) Risks for Adults and Children across Fumarolic Vents

The upper panel of Figure 2 shows that HQ values for adults ranged between 0.15 and 0.50 across fumaroles, all below the USEPA (2011) threshold of 1, implying negligible non-cancer health risks. In contrast, HQ values for children vary from 0.30 to 0.98, approaching the critical limit at fumaroles F9 and F10. These vents correspond to the inner caldera, where elevated temperatures ($>73\text{ }^{\circ}\text{C}$) and vigorous vapor flux enhance rock–steam interactions, thereby promoting the leaching and volatilization of arsenic and cadmium from hydrothermally altered rocks. Similar processes have been reported in other geothermal fields, where higher vent temperatures and vapor-dominated systems accelerate trace-metal mobilization into condensates (Durowoju et al., 2020; Fahimah et al., 2024).

The spatial trend indicates a progressive increase in HQ from peripheral vents (F1–F6) toward the inner caldera (F8–F10). This pattern mirrors the geothermal intensity gradient and confirms that elevated fumarolic temperatures amplify heavy-metal transfer into vapor condensates, as observed in comparable high-enthalpy geothermal environments (Durowoju et al., 2020). The mean HQ and cumulative HI values—0.36 for adults and 0.80 for children—further reaffirm that although current exposure levels remain within acceptable limits, children residing near hot vents face marginal, but notable non-carcinogenic risks associated with geogenic arsenic and cadmium emissions.

Carcinogenic Health Risk

Lifetime Cancer Risk (LCR) values were computed for arsenic and cadmium using USEPA (2011) slope factors of 1.5 and 6.3 ($\text{mg kg}^{-1} \text{ day}^{-1}$)⁻¹, respectively. For adults, total LCR ranged between 4.1×10^{-5} and 2.1×10^{-4} (mean = 7.6×10^{-5}), while for children, it varied from 1.9×10^{-5} to 9.8×10^{-5} (mean = 1.8×10^{-4}). These values fall within or slightly above the USEPA's acceptable range (10^{-6} – 10^{-4}), consistent with recent studies reporting similar risk magnitudes for waterborne arsenic and cadmium exposure in geothermal and hydrothermal environments (Saber et al., 2024).

The highest LCR values were observed in fumaroles F9 and F10 (inner caldera), where elevated temperatures ($>73\text{ }^{\circ}\text{C}$) and strong vapor discharge likely enhance volatilization and partitioning of arsenic and cadmium into condensate fluids. Processes of temperature-driven leaching and magmatic fluid input have been shown in geothermal systems to elevate trace-metal burdens in high-temp fluids (Saby et al., 2024)

The highest LCR values were observed at fumaroles F9 and F10 (inner caldera), where elevated temperatures ($>73\text{ }^{\circ}\text{C}$) and intense vapor discharge likely enhance the volatilization and partitioning of arsenic and cadmium into condensate. This aligns with findings from geothermal settings demonstrating that high-temperature zones promote trace-metal mobilization and gas–water exchange (Taufiq, 2023).

CONCLUSION

The study establishes that fumarolic condensates from the Mt. Suswa geothermal field exhibit low to moderate heavy-metal enrichment largely controlled by geothermal intensity and rock–steam interactions. The concentrations of arsenic (2.24–5.49 ppb), lead (0.95–1.98 ppb), and cadmium (0.39–1.41 ppb) were well below the WHO (2022) and NEMA (2024) limits for potable water, confirming the condensates' acceptable chemical quality.

Spatial variability indicates that vents within the inner caldera (F9–F10) recorded the highest As and Cd concentrations, corresponding to zones of elevated temperature and vapor flux that enhance metal volatilization from hydrothermally altered rocks.

Health-risk assessment revealed that non-carcinogenic risks ($\text{HQ} < 1$) are negligible for adults and marginal for children, while carcinogenic risks ($\text{LCR} \approx 10^{-5}$ – 10^{-4}) remain within or slightly above the USEPA acceptable range. Generally, fumarolic condensates from Mt. Suswa are safe for limited domestic use but require periodic monitoring and local mitigation such as point-of-use treatment (bone char or activated alumina) and community awareness to minimize exposure in high-temperature vent areas.

ACKNOWLEDGMENTS

The author expresses sincere gratitude to Prof. Kitetu Kitetu and Dr. Carolyn Chepkirui of Kabarak University School of Science, Engineering and Technology for their invaluable contribution throughout this research. The cooperation of the Mt. Suswa local community during field sampling is deeply acknowledged.

Conflict of Interest

The authors affirm their complete impartiality, declaring that no conflicts of interest exist, thereby reinforcing the credibility, transparency, and integrity of the research findings.

Ethical Approval

Ethical approval for this study was obtained from the Kabarak University Ethics Review Committee (KUERC) in accordance with national research ethics guidelines. The approval covered both environmental sampling and the administration of household surveys involving human participants. Research authorization was subsequently granted by the National Commission for Science, Technology and Innovation (NACOSTI) under license number NACOSTI/P/25/4176440, permitting fieldwork within the Mt. Suswa study area.

Data Availability

The datasets generated and analyzed during this study (physico-chemical parameters, heavy-metal concentrations, HQ/HI/LCR indices, and geospatial coordinates) are available from the corresponding author upon reasonable request.

Supplementary materials, analytical calibration curves, and raw instrumental data have been archived with the Kabarak University Institutional Repository for academic reference.

REFERENCES

1. Augusto, M., Lamberti, M. C., Tassi, F., Carbajal, F., Llano, J., Nogués, V., Núñez, N., Sánchez, H., Rizzo, A., García, S., Yiries, J., Vélez, M. L., Massenzio, A., Velasquez, G., Bucarey, C., Gómez, M., Euillades, P., & Ramos, V. (2023). Eleven-Year Survey of the Magmatic-Hydrothermal Fluids From Peteroa Volcano: Identifying Precursory Signals of the 2018–2019 Eruption. *Geochemistry, Geophysics, Geosystems*, 24(11), 1–19. <https://doi.org/10.1029/2023GC011064>
2. Ahmed, T., Sarwar, B. A., Sultana, R., & Akhtar, S. (2023). Application of Heavy Metal Pollution Index (HPI) for Assessment of Drinking Water Quality in Islamabad. *Research Square*, 1(2), 1–15.
3. Anitha, B. H., Maya Naik, S. N., Nanjundaswamy, C., & Divyanand, M. S. (2021). Application of Heavy Metal Pollution Index and Metal Index for the Assessment of Groundwater Quality in Peenya Industrial Area. *IOP Conference Series: Earth and Environmental Science*, 822(1). <https://doi.org/10.1088/1755-1315/822/1/012033>
4. APHA. (2022). *Standard Methods for the Examination of Water and Wastewater* (24th ed.), Washington, DC, USA: American Public Health Association. Standard Methods for the Examination of Water and Wastewater, 23rd edition, 1–1545. <https://doi.org/10.2105/SMWW.2882.216>
5. Ayari, J., Barbieri, M., Boschetti, T., Barhoumi, A., Sellami, A., Braham, A., Manai, F., Dhaha, F., & Charef, A. (2023). Major- and Trace-Element Geochemistry of Geothermal Water from the Nappe Zone, Northern Tunisia: Implications for Mineral Prospecting and Health Risk Assessment. *Environments - MDPI*, 10(9). <https://doi.org/10.3390/environments10090151>
6. Ayaz, H., Nawaz, R., Nasim, I., Irshad, M. A., Irfan, A., Khurshid, I., Okla, M. K., Wondmie, G. F., Ahmed, Z., & Bourhia, M. (2023). Comprehensive human health risk assessment of heavy metal contamination in urban soils: insights from selected metropolitan zones. *Frontiers in Environmental Science*, 11(December), 1–17. <https://doi.org/10.3389/fenvs.2023.1260317>
7. Badeenezhad, A., Soleimani, H., Shahsavani, S., Parseh, I., Mohammadpour, A., Azadbakht, O., Javanmardi, P., Faraji, H., & Babakrpur Nalosi, K. (2023). Comprehensive health risk analysis of heavy metal pollution using water quality indices and Monte Carlo simulation in R software. *Scientific Reports*,

- 13(1), 1–18. <https://doi.org/10.1038/s41598-023-43161-3>
8. Bair, E. C. (2022). A Narrative Review of Toxic Heavy Metal Content of Infant and Toddler Foods and Evaluation of United States Policy. *Frontiers in Nutrition*, 9(June), 1–9. <https://doi.org/10.3389/fnut.2022.919913>
9. Biedunkova, O., & Kuznietsov, P. (2024). Dataset on heavy metal pollution assessment in freshwater ecosystems. *Scientific Data*, 1–11. <https://doi.org/10.1038/s41597-024-04116-z>
10. Brraich, O. S., & Jassal, R. (2021). Evaluation of Water Quality Pollution Indices for Heavy Metal Contamination Monitoring in Surface Water of Sutlej River (India). *Toxicology International*, 28(4), 327–335. <https://doi.org/10.18311/ti/2021/v28i4/27421>
11. Campeny, M., Menéndez, I., Ibáñez-Insa, J., Rivera-Martínez, J., Yepes, J., Álvarez-Pousa, S., Méndez-Ramos, J., & Mangas, J. (2023). The ephemeral fumarolic mineralization of the 2021 Tajogaite volcanic eruption (La Palma, Canary Islands, Spain). *Scientific Reports*, 13(1), 1–14. <https://doi.org/10.1038/s41598-023-33387-6>
12. Capitão, C., Martins Raquel, Snatos Osvaldo, Bicho Manuel, Szigeti Tamás, Katsonouri Andromachi, Bocca Beatrice, Ruggieri Flavia, Wasowicz Wojciech, Tolonen Hanna, & Virgolino Ana. (2022). Exposure to heavy metals and red blood cell parameters in children: A systematic review of observational studies. *Frontiers in Pediatrics*.
13. Charkiewicz, A. E., Omeljaniuk, W. J., Nowak, K., Garley, M., & Nikliński, J. (2023). Cadmium Toxicity and Health Effects—A Brief Summary. *Molecules*, 28(18), 1–16. <https://doi.org/10.3390/molecules28186620>
14. Demissie, S., Mekonen, S., Awoke, T., Teshome, B., & Mengistie, B. (2024). Examining carcinogenic and noncarcinogenic health risks related to arsenic exposure in Ethiopia: A longitudinal study. *Toxicology Reports*, 12(January), 100–110. <https://doi.org/10.1016/j.toxrep.2024.01.001>
15. Durowoju, O. S., Ekosse, G. I. E., & Odiyo, J. O. (2020). Occurrence and health-risk assessment of trace metals in geothermal springs within Soutpansberg, Limpopo Province, South Africa. *International Journal of Environmental Research and Public Health*, 17(12), 1–20. <https://doi.org/10.3390/ijerph17124438>
16. Elbarbary, S., Abdel Zaher, M., Saibi, H., Fowler, A. R., & Saibi, K. (2022). Geothermal renewable energy prospects of the African continent using GIS. *Geothermal Energy*, 10(1), 1–19. <https://doi.org/10.1186/s40517-022-00219-1>
17. Eldaw, E., Huang, T., Elubid, B., Mahamed, A. K., & Mahama, Y. (2020). A novel approach for indexing heavy metals pollution to assess groundwater quality for drinking purposes. *International Journal of Environmental Research and Public Health*, 17(4), 1–16. <https://doi.org/10.3390/ijerph17041245>
18. Fahimah, N., Salami, I. R. S., Oginawati, K., & Mubiarto, H. (2024). Appraisal of pollution levels and non-carcinogenic health risks associated with the emergence of heavy metals in Indonesian community water for sanitation, hygiene, and consumption. *Emerging Contaminants*, 10(3), 100313. <https://doi.org/10.1016/j.emcon.2024.100313>
19. Gantayat, R. R., Elumalai, V., Li, P., Patience, M. T., & Wolff-Boenisch, D. (2025). Comprehensive Source Apportionment and Health Risk Assessment of Metals Contamination with Unified Approach of Receptor Model and Monte Carlo Simulation in Limpopo, South Africa. *Exposure and Health*, 0123456789. <https://doi.org/10.1007/s12403-025-00734-z>
20. Inostroza, M., Moune, S., Moretti, R., Robert, V., Bonifacie, M., Chilin-Eusebe, E., Burtin, A., & Burckel, P. (2022). Monitoring Hydrothermal Activity Using Major and Trace Elements in Low-Temperature Fumarolic Condensates: The Case of La Soufriere de Guadeloupe Volcano. *Geosciences (Switzerland)*, 12(7). <https://doi.org/10.3390/geosciences12070267>
21. Jadoon, I., Ahmad, K., Nazir, A., Khan, S. A., Ismail, A. M., Matar, A., Alharbi, A. S., & Saleh, H. A. F. (2025). Health risk assessment and levels of heavy metals contaminated drinking water used by both adults and children from Nawanshahr town. *Global Nest Journal*, 27(4). <https://doi.org/10.30955/gnj.07139>
22. kaur, R., Garkal, A., Sarode, L., Bangar, P., Mehta, T., Singh, D. P., & Rawal, R. (2024). Understanding arsenic toxicity: Implications for environmental exposure and human health. *Journal of Hazardous Materials Letters*, 5(August 2023), 100090. <https://doi.org/10.1016/j.hazl.2023.100090>
23. Kowalska, J. B., Mazurek, R., Gąsiorek, M., & Zaleski, T. (2018). Pollution indices as useful tools for the comprehensive evaluation of the degree of soil contamination—A review. *Environmental Geochemistry and Health*, 40(6), 2395–2420. <https://doi.org/10.1007/s10653-018-0106-z>
24. Kumar, S., & Maurya, N. S. (2025). Analysis of heavy metal contamination in groundwater and associated

- probabilistic human health risk assessment using Monte Carlo simulation: A case study in Gaya, Bihar. *Journal of Water and Health*, 23(5), 630–647. <https://doi.org/10.2166/wh.2025.348>
25. Mangi, P. (2016). Geothermal exploration and utilization in Kenya. Table 1, 1–11.
26. Masikonte, L. N. (2020). Potential Environmental and Socio-economic Effects of Geothermal Exploitation on the Local Community: a Case of Suswa Geothermal Plant.
27. Mohamud, Y. N. (2013). 1D Joint Inversion of TEM and MT Data : Suswa Geothermal Field, Rift Valley, Kenya. 19.
28. Morales-deAvila, H., Gutiérrez, M., Colmenero-Chacón, C. P., Júnez-Ferreira, H. E., & Esteller-Alberich, M. V. (2023). Upward Trends and Lithological and Climatic Controls of Groundwater Arsenic, Fluoride, and Nitrate in Central Mexico. *Minerals*, 13(9). <https://doi.org/10.3390/min13091145>
29. Mukwevho, N., Mabowa, M. H., Ntsasa, N., Mkhohlakali, A., Chimuka, L., Tshilongo, J., & Letsoalo, M. R. (2025). Seasonal Pollution Levels and Heavy Metal Contamination in the Jukskei River, South Africa. *Applied Sciences (Switzerland)*, 15(6), 1–20. <https://doi.org/10.3390/app15063117>
30. NEMA. (2024). Environmental Management and Co-ordination (Water Quality) Regulations. Kenya Gazette Supplement No. 68, 177, 1–25.
31. Nyairo, B., Shako, L., & Mutia, T. (2014). Environmental suitability analysis for geothermal development: A case study for suswa geothermal prospect, Kenya. *Transactions - Geothermal Resources Council*, 38, 865–869.
32. Obase, T., Sumino, H., Toyama, K., Kawana, K., Yamane, K., Yaguchi, M., Terada, A., & Ohba, T. (2022). Monitoring of magmatic–hydrothermal system by noble gas and carbon isotopic compositions of fumarolic gases. *Scientific Reports*, 12(1), 1–12. <https://doi.org/10.1038/s41598-022-22280-3>
33. Okoro, H. K., Orosun, M. M., Agboola, A. F., Emenike, E. C., Nanduri, S., Kedia, N., Kariem, M., Priya, A., & Rab, S. O. (2025). Health risk assessments of heavy metals in dust samples collected from classrooms in Ilorin, Nigeria and its impact on public health. *Heliyon*, 11(4), e42769. <https://doi.org/10.1016/j.heliyon.2025.e42769>
34. Prasad, B., & Bose, J. M. (2001). Evaluation of the heavy metal pollution index for surface and spring water near a limestone mining area of the lower himalayas. *Environmental Geology*, 41(1–2), 183–188. <https://doi.org/10.1007/s002540100380>
35. Raad, H. F., Pardakhti, A., & Kalarestaghi, H. (2021). Carcinogenic and Non carcinogenic Health Risk Assessment of Heavy Metals in Ground Drinking Water Wells of Bandar Abbas. *Pollution*, 7(2), 395–404. <https://doi.org/10.22059/poll.2021.317359.995>
36. Saber, A. A., Al-Mashhadany, M. F. M., Hamid, A., Gabrieli, J., Tockner, K., Alsaif, S. S. A., Al-Marakeby, A. A. M., Segadelli, S., Cantonati, M., & Bhat, S. U. (2024). Carcinogenic and Non-Carcinogenic Health Risk Evaluation of Heavy Metals in Water Sources of the Nubian Sandstone Aquifer in the El-Farafra Oasis (Egypt). *Water (Switzerland)*, 16(12). <https://doi.org/10.3390/w16121649>
37. Saby, M., van Hinsberg, V., Pinti, D. L., Berlo, K., Gautason, B., Sigurðardóttir, Á., & Castro, M. C. (2024). Magmatic and rock-leaching contributions to the metal load in hydrothermal fluids at Þeistareykir, Iceland. *Applied Geochemistry*, 176(October). <https://doi.org/10.1016/j.apgeochem.2024.106213>
38. Sanjuan, B. (2024). Auxiliary Chemical Geothermometers Applied to Waters from Some East African Rift Areas (Djibouti, Ethiopia, Kenya) for Geothermal Exploration. *Petroleum and Chemical Industry International*, 7(4), 01–12. <https://doi.org/10.33140/pcii.07.04.01>
39. Shetty, B. R., Pai, B. J., Salmataj, S. A., & Naik, N. (2024). Assessment of Carcinogenic and non-carcinogenic risk indices of heavy metal exposure in different age groups using Monte Carlo Simulation Approach. *Scientific Reports*, 14(1), 1–20. <https://doi.org/10.1038/s41598-024-81109-3>
40. Sunguti, A. E., Kibet, J. K., Kinyanjui, T. K., Oyugi, A. M., & Muhizi, T. (2024). The analysis of potentially toxic heavy metal contamination in the Lake Bogoria geothermal springs. *Discover Toxicology*, 1(1). <https://doi.org/10.1007/s44339-024-00003-9>
41. Taufiq, T. (2023). Arsenic Gas on Geothermal Area, Part III: Case Study and Correlation with Temperature. *EAGE Conference on the Future of Energy - Role of Geoscience in the Energy Transition*, 25–28. <https://doi.org/10.3997/2214-4609.202372032>
42. Tokatli, C. (2024). AN APPLICATION OF HEAVY METAL POLLUTION INDEX AND HEAVY METAL EVALUATION INDEX TO EVALUATE THE WATER QUALITY OF ATIKHISAR DAM. November.
43. USEPA. (2011). Exposure Factors Handbook: 2011 Edition. U.S. Environmental Protection Agency,

- EPA/600/R-(September), 1–1466. <https://doi.org/EPA/600/R-090/052F>
44. Werner, C. A., Kern, C., & Kelly, P. J. (2020). Chemical Evaluation of Water and Gases Collected from Hydrothermal Systems Located in the Central Aleutian Arc, August 2015. USGS Scientific Investigations Report, 2020–5043(August 2015), 35 p.
45. WHO. (2022). Guidelines for drinking-water quality: Fourth edition incorporating the first and second addenda. In ReVision (Vol. 21, Issue 6).
46. Wu, H., Wang, X., Ren, H., Gao, M., Cai, J., & Cheng, J. (2024). Groundwater Heavy Metal Pollution Characteristics and Health Risk Assessment in Typical Industrial Parks in Southwest China. *Water (Switzerland)*, 16(23), 1–23. <https://doi.org/10.3390/w16233435>
47. Yaguchi, M., Ohba, T., & Kanno, S. (2025). mber 2024Geochemical evaluation for the fumarolic gases collected at Ojigokudani, Iwate volcano, Japan in Septe. *Earth, Planets and Space*, 77(1). <https://doi.org/10.1186/s40623-025-02260-3>
48. Yao, B., Zhou, X., Qiu, D., Du, J., He, M., Tian, J., Zeng, Z., Wang, Y., Yan, Y., Xing, G., Cui, S., Li, J., Dong, J., Li, Y., & Zhang, F. (2024). Geochemical Characteristics of Trace Elements of Hot Springs in the Xianshuihe–Xiaojiang Fault Zone. *Water (Switzerland)*, 16(5). <https://doi.org/10.3390/w16050680>